

ESA Cloud_cci+

Climate Assessment Report



Issue 1 Revision 0

25/09/2023

Deliverable No.: D-5.1

ESRIN/Contract No.: 4000128637/20/I-NB

Science lead: Dr. Martin Stengel

Deutscher Wetterdienst martin.stengel@dwd.de

Technical Officer: Michael Eisinger

European Space Agency michael.eisinger@esa.int





Doc:				Cloud_cci+_D5.1_CAR_v1.0.docx
Date:				25/09/2023
Issue:	1	Revision:	0	Page 2

Document Change Record

Document, Version	Date	Changes	Originator
v1.0 submitted	25/09/2023	Initial Version	M. Stengel
v1.0	25/09/2023	Issued Version	M. Stengel

Purpose

The purpose of this document is to demonstrate how Cloud_cci+ data can be used in climate science applications. This is done on an exemplary basis by (a) summarizing the results of the two User Case Studies conducted in Cloud_cci+ Phase I and (b) reporting the additional developments done for a simplistic satellite simulator and selected comparisons between ERA-5 and SLSTR data.



Doc:				Cloud_cci+_D5.1_CAR_v1.0.docx
Date:				25/09/2023
Issue:	1	Revision:	0	Page 3

Contents

	SER CASE STUDY I - A LAGRANGIAN PERSPECTIVE ON THE LIFECYCLE AND CLO ATIVE EFFECT OF DEEP CONVECTIVE CLOUDS OVER AFRICA	
1.1	Scope	4
1.2	Summary	4
	SER CASE STUDY II - DESIGNING A 'SUNNY VACATION MAP' BASED ON SATELL RVATIONS ON CLOUDS AND RADIATION	
2.1	Scope	7
2.2	Data basis	7
2.3	Approach	7
2.4	Summary of results	7
3 S	IMPLIFIED SIMULATOR	9
	Background	
3.2	Adaptation in Cloud_cci+ Phase I	.10
3.3	Summary of results	.10
4 D	EFINITIONS, ACRONYMS, ABBREVIATIONS	.14
DEEE	DENCES.	16

	Doc:				Cloud_cci+_D5.1_CAR_v1.0.docx
cloud	Date:				25/09/2023
cci	Issue:	1	Revision:	0	Page 4

1 User Case Study I - A Lagrangian Perspective on the Lifecycle and Cloud Radiative Effect of Deep Convective Clouds Over Africa

The report in this section is a brief summary of Jones et al. (2023).

1.1 Scope

In this study cloud and radiative flux properties from the Cloud_cci+ SEVIRI dataset was utilized. In a 4 month period, deep convective systems (DCCs) are identified, tracked and their life cycle investigated with respect to the top-of-atmosphere cloud radiative effect of their anvil clouds. Their cumulative effects are analysed and put in relation of the (a) initiation time of the DCCs, (b) their lifetime, and (c) the number of core a DCC has.

1.2 Summary

Figure 1-1 shows the frequency of detected convective cores. Figure 1-2 shows the net cloud radiative effect and its components for three selected cases:

- a) A rather short-lived DCC which is initiated in the afternoon and which dissipates in the early evening. This DCC has a negative cumulative radiative effect (cooling)
- b) A DCC that exists almost 24 hours into the morning of the next day. This DCC has a positive cloud radiative effect (warming)
- c) A clustered DCC that had multiple cores and lived several days. The cumulative cloud radiative effect of this system is very close to zero.

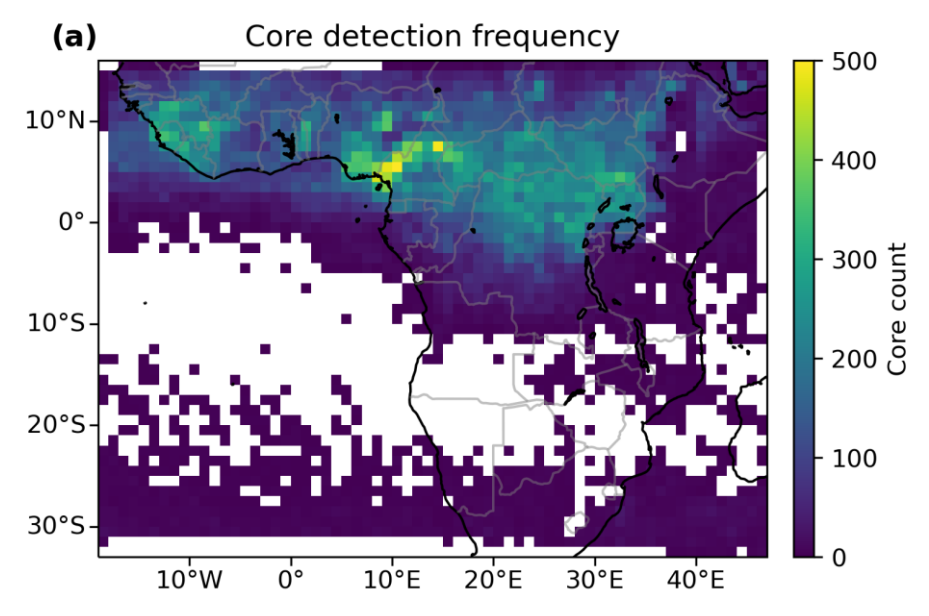
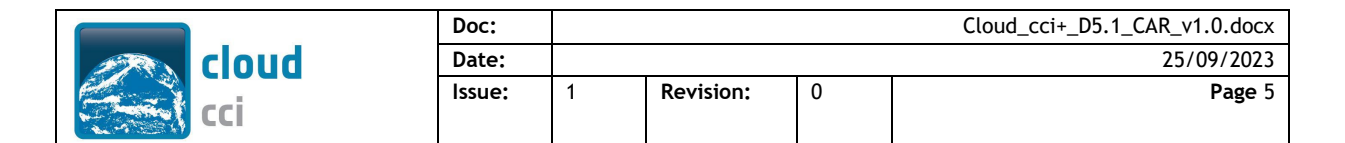


Figure 1-1 Number of detected cores (a) and average hour of core detection (b) by 1x1° grid box. Grid boxes in (b) with a standard deviation greater than 6 hours are single-hatched, and greater than 12 hours cross-hatched. Figure and caption taken from Jones et al. (2023).

Figure 1-3 shows the histogram over the mean cloud radiative effect of all track DCCs in the 4 month period. It depicts that there is a bimodal distribution with the first mode peaking around -200 Wm⁻² (cooling) composed of the short-lived single-core DCCs. The second mode peaking around 100 Wm⁻² (warming) is composed of the longer-living DCCs. However, the mean cloud radiative of the clustered multi-core DCC is around 0 Wm⁻². And interestingly, the mean cloud radiative effects over all DCCs is



also close to zero, despite the two modes. The later confirms the common assumption that Tropical DCCs have a nearly neutral effects on the top of atmosphere radiative budget.

More information on this study can be found in Jones et al. (2023).

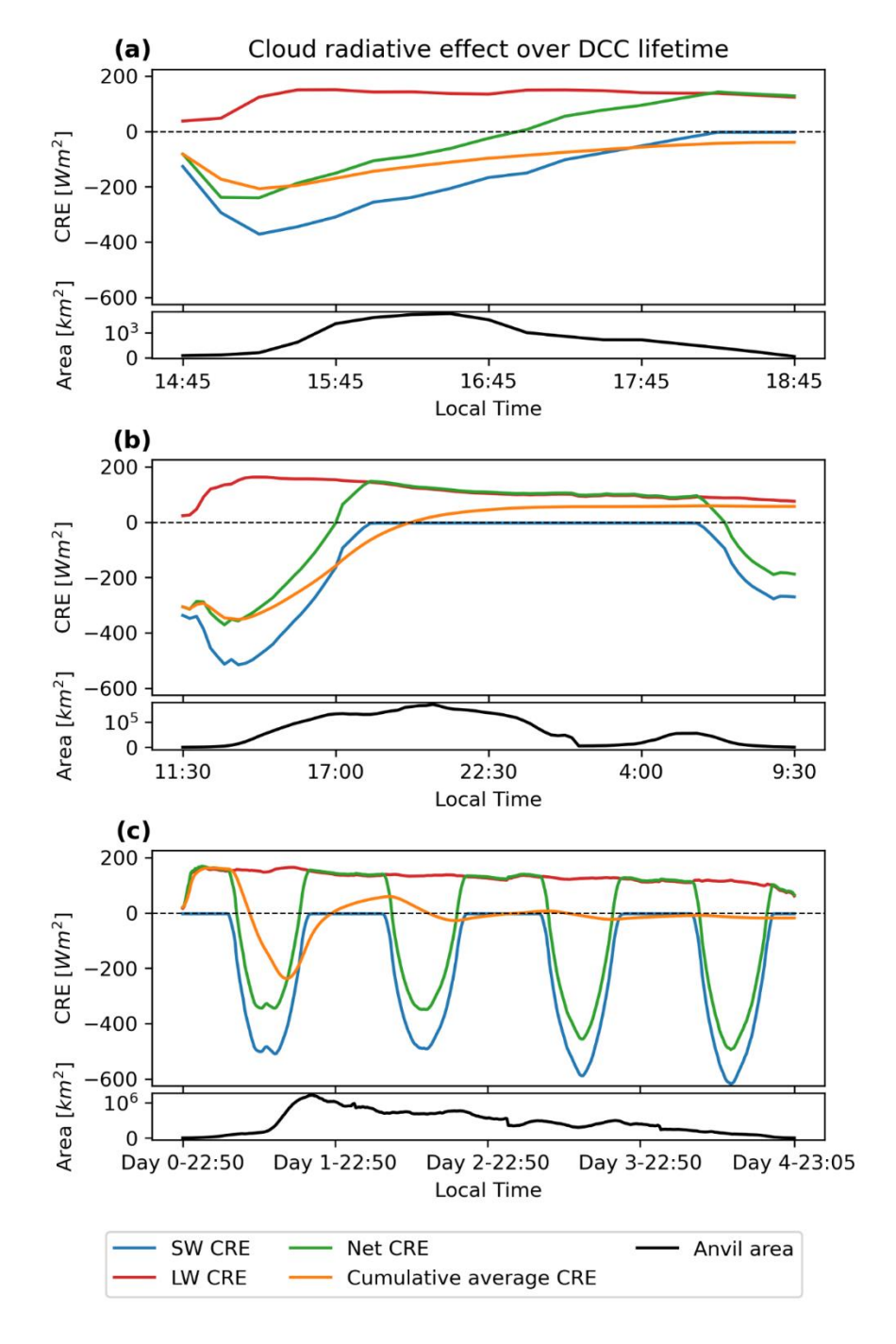


Figure 1-2 Anvil net, LW, and SW CRE, accumulated mean CRE over anvil lifetime and anvil area for (a) an isolated, short-lived (4-hour) DCC, (b)a moderately clustered, 1-day long DCC, and (c) a large, clustered, 4-day long DCC. All times are the local solar time, to the nearest 5 minute interval. Figure and caption taken from **Jones et al.** (2023).



Doc:				Cloud_cci+_D5.1_CAR_v1.0.docx
Date:				25/09/2023
Issue:	1	Revision:	0	Page 6

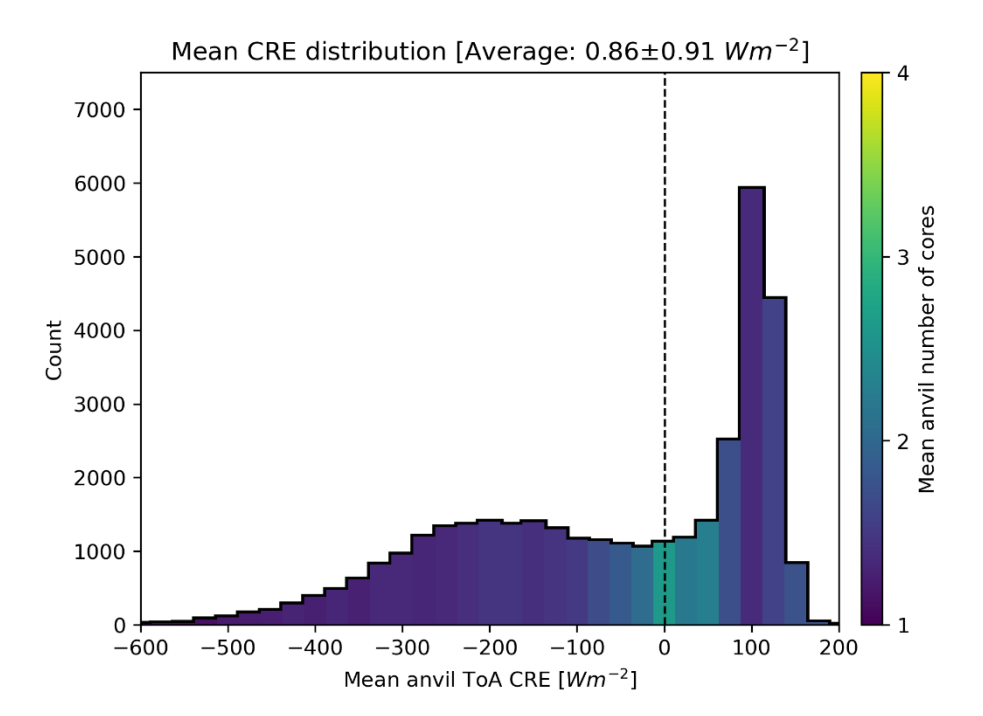


Figure 1-3 The distribution of lifetime anvil CRE for all observed anvils. The mean number of cores per anvil in each bin is indicated by the colour scale. The vertical dashed line shows the integrated mean CRE over all anvils, weighted by the anvil areas (0.86±0.91 Wm⁻²). Figure and caption taken from **Jones et al. (2023)**.



Doc:				Cloud_cci+_D5.1_CAR_v1.0.docx
Date:				25/09/2023
Issue:	1	Revision:	0	Page 7

2 User Case Study II - Designing a 'Sunny Vacation Map' based on Satellite Observations on Clouds and Radiation

The report in this section is a summary of RUCS2.

2.1 Scope

This study highlights a specific aspect of how long-term satellite observations of cloud and radiation properties facilitate real-life applications. Having more than three decades of those observations available provides a very sound basis for a statistical analysis of not only the occurrence of sunny days (more or less the inverse of cloud fraction), but also how these are clustered.

In this report the determination of sunny days is described and how sunny periods are defined as function of the sunny day sequences. Global maps of the likelihood of sunny periods are shown, stratified by season, and discussed.

In addition, two pairs of European cities were selected to compare the general likelihood of sunny periods and elaborate on the temporal evolution of this information throughout the whole time series.

This study is considered as teaser for a potential operational application.

2.2 Data basis

Basis of our analysis is the Cloud_cci AVHRR-PMv3 dataset (Stengel et al., 2020), compiled within ESA's Cloud Climate Change Initiative (Cloud_cci) Phase 2. It is a global dataset on clouds and radiation covering the period of 1982 to 2016, which results in a long-term data record of 35 years - long enough to consider it a climatology.

Cloud and radiation properties were retrieved from passive remote sensing measurements recorded by the Advanced Very High Resolution Radiometer (AVHRR) - in particular by those flying on afternoon (PM) polar orbiting satellites of the National Oceanic and Atmospheric Administration (NOAA). They encircle the Earth from pole to pole about a dozen times per day, gathering information from all around the globe. PM satellites are those satellites that have an equator crossing time in the afternoon (local solar time). See Fehler! Verweisquelle konnte nicht gefunden werden. for an overview of all satellites included and their respective equator crossing times.

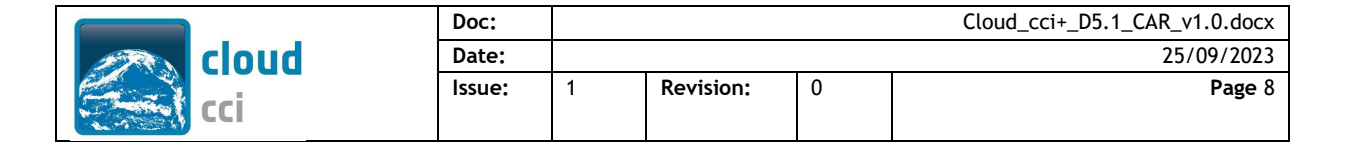
2.3 Approach

The likelihood of a sunny period is here defined as the probability to get at least "x" days of sunshine within a total amount of "n" days of vacation, which might be one of the most valuable information for a holiday maker.

Sunny days are days for which the ratio of obtained to possible shortwave radiation being bigger than 0.85 (and for "cloudy" being smaller than 0.85).

2.4 Summary of results

As an example result, Figure 2-1 illustrates the results of our global analysis, the global "sunny vacation map" of sunny periods: It gives the likelihood to get at least 5 sunny days within 7 days of vacation lying ahead, spatially resolved on global scale (albeit slightly coarser than possible, see above) and depending on the time of the year. Oceanic regions are masked out as the typical holiday resort is on land, unless it is a sailing trip or cruise. The map reveals that, globally seen, the whole range of possible probabilities for sunny periods is covered, ranging from nearly 0% in e.g. the inner tropics near the equator to almost 100% in desert regions like the Sahara. Primarily, the probability for sunny periods varies with latitude. It is generally large (more than 60% in the mean) in the subtropics, where large-scale subsidence typically supresses the formation of clouds. It is rather small



(less than 20% in the mean) in the outer tropics, where strong insolation triggers intense cloud formation. And it is moderate (between 10 to 40%) in the mid-latitudes, where highs and lows frequently alternate, usually bringing a diverse mix of sun and clouds.

More information on this User Case Study can be found in RUCS2.

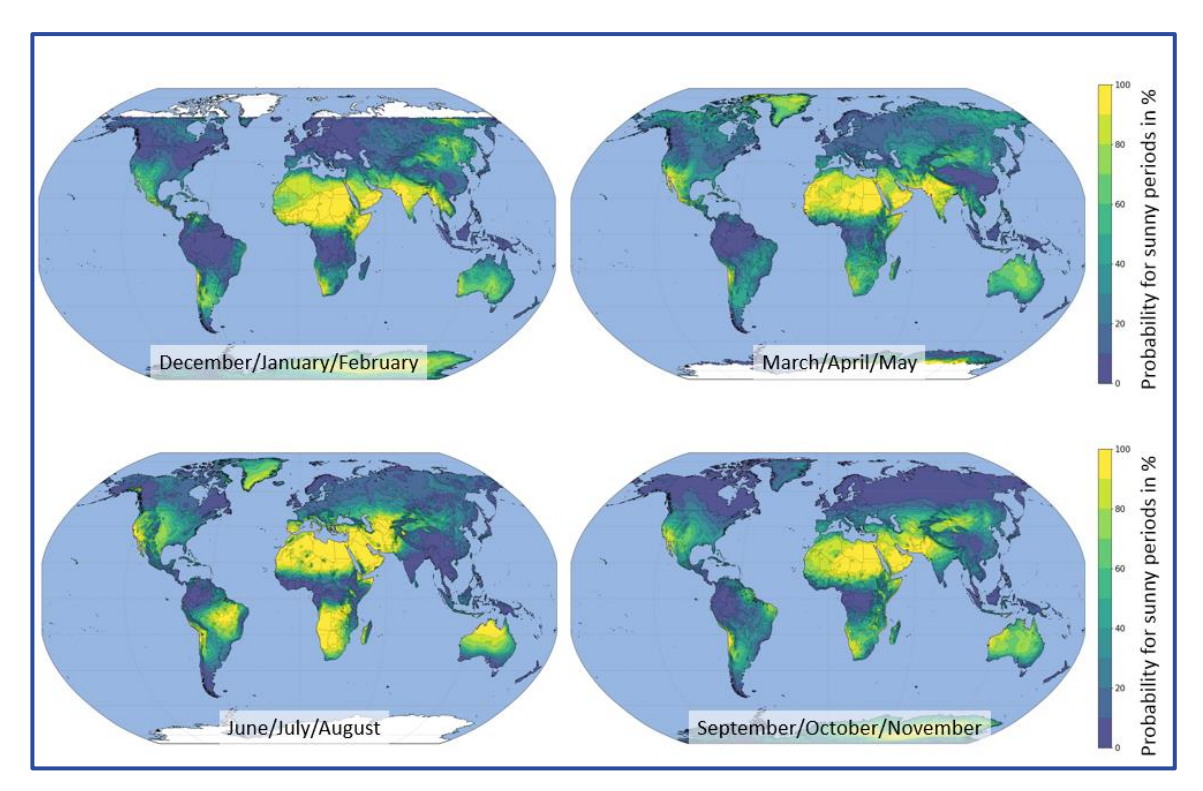


Figure 2-1 Global "sunny vacation map" of sunny periods



Doc:				Cloud_cci+_D5.1_CAR_v1.0.docx
Date:				25/09/2023
Issue:	1	Revision:	0	Page 9

3 Simplified Simulator

3.1 Background

3.1.1 Simplistic cloud simulator for ERA-Interim

A full and peer-reviewed description of the simplistic cloud simulator is given in Stengel et al. (2018). The purpose of the SIMplistic cloud simulator For ERA-Interim (SIMFERA) developed in the framework of ESA Cloud_cci is to evaluate the cloud parameterization used in ECMWF models, although SIMFERA is assumed to be applicable to other model data too. In general SIMFERA consists of three modules: (1) downscaler, which converts the model grid box mean profiles into sub-grid profiles considering the mismatch in spatial scale between that of a model and that of a satellite pixel; (2) pseudoretrieval, which emulates the pixel-scale cloud parameters based on the sub-grid profiles; and (3) statistical aggregation, which builds the diagnostic output that is comparable to the observational dataset (i.e. temporal averages and histograms, see below).

The general features are:

- SIMFERA uses the three-dimensional (3D) model fields as input (see details below). The simplistic approach in offline mode has the advantage of short computation time (e.g. 33 years of reanalysis data processed in less than 2 days on a HPC system).
- Unlike sophisticated simulators, which are using modelled radiances and brightness temperatures to retrieve cloud optical parameters based on radiative transfer calculations (e.g., COT and CER following Nakajima-King method), SIMFERA stays very close to the original model fields. For instance, it uses the ERA-Interim CER parameterization (Martin et al. 1994, Sun and Rikus 1999, Sun 2001) along with the original 3D variables to convert the model state into comparable synthetic observations. Details are given in Stengel et al. (2017c).
- No satellite overpass is taken into account as ERA-Interim is only available in discrete temporal resolution of several hours. However, day and night conditions are considered for the calculation of cloud optical parameters (i.e. COT, CER, CWP) that are only available during daytime observations since they are based on visible measurements.
- SIMFERA provides 2 options about how liquid and ice clouds occurring in the same model grid box are treated during the simulations (in the sub-column procedure): mixed phase (i.e. mixed phase clouds if both water/ice contents exists) or no-mixed phase (i.e. considering liquid and ice clouds separately).
- SIMFERA can be used for other model output evaluation after small modifications since there are not instrument/algorithm specifications implemented.

Input:

The simulator reads 6-hourly (00, 06, 12, 18 UTC) gridded estimates of 3D meteorological upper air parameters on 60 model levels including the following profiles: liquid water content "LWC" [kg/kg], ice water content "IWC" [kg/kg], cloud cover "CC" (0-1), temperature "T" [K], and specific humidity "Q" [kg/kg].

Additionally, the ERA-Interim file comprises for each grid box two-dimensional (2D) arrays of surface geopotential "Z" $[m^2/s^2]$ an logarithm of surface pressure "LNSP" [Pa].

The latter two parameters are required for the computation of vertical pressure and geopotential profiles by using the provided "A" and "B" coefficients on model levels along with T and Q profiles.

Output:

Grid box monthly means are computed averaging first over all sub-columns per grid box and then averaging over all diagnostic time steps per month. Histograms are based on sub-column values because the downscaled results mimic the spatial resolution of a satellite footprint.



Doc:				Cloud_cci+_D5.1_CAR_v1.0.docx
Date:				25/09/2023
Issue:	1	Revision:	0	Page 10

SIMFERA provides the following monthly mean products: total, high-, mid-, and low-level CFC (0-1), CPH (0-1), LWP and IWP [g/m²],CTP [hPa], CTH [km], and CTT [K], COT and CER [micron] for liquid and ice phase, 2D joint cloud property histograms following the ISCCP classification relating the simulated height and optical thickness of the clouds, and 1D histograms for CTP, CTT, CWP, COT, and CER with the cloud phase as additional dimension.

3.2 Adaptation in Cloud_cci+ Phase I

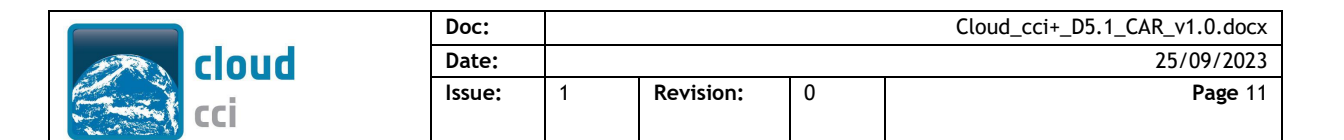
The following developments were done in Cloud_cci+ Phase I.

- Replacing ERA-Interim by ERA-5 as input, including increasing horizontal resolution from 1.0° to 0.5° and increasing the vertical resolution from 60 model levels to 137 model levels
- Increasing number of sub-columns in the simulator from 20 to 40 (approx.. representing ~1km spatial resolution)
- · Applying SIMFERA to the entire year of 2019
- Aggregating to 0.5 L3C products (comparable to Cloud_cci+ SLSTR L3C)
- Porting the entire source code and processing environment to new ECMWF computer facilities (ATOS)

These tasks were not only done to update SIMFERA but also to adapt it to the SLSTR data processed in Cloud_cci+ Phase I. In the next section the results of a brief comparison between SIMFERA and SLSTR S3a data for 2019 are shown.

3.3 Summary of results

The SLSTR data referred to in this subsection are the Cloud_cci+ Phase I SLSTR S3a data version 3, for July 2019. Fehler! Verweisquelle konnte nicht gefunden werden. shows maps and zonal means of monthly mean cloud fraction from SLSTR and ERA-5 SIMFERA results, and the latter for three different COT thresholds. Generally ERA-5 shows good agreements with SLSTR between 60S and 60N with only small sensitivity to the applied COT threshold. In the high latitudesERA-5 has much more cloudiness than SLSTR when all clouds are considered. However, removing the thinnest clouds clearly increases the agreement in the Southern high latitudes. In the Northern high latitudes however, the ERA-5 cloud fraction shows only small change in these scenarios.



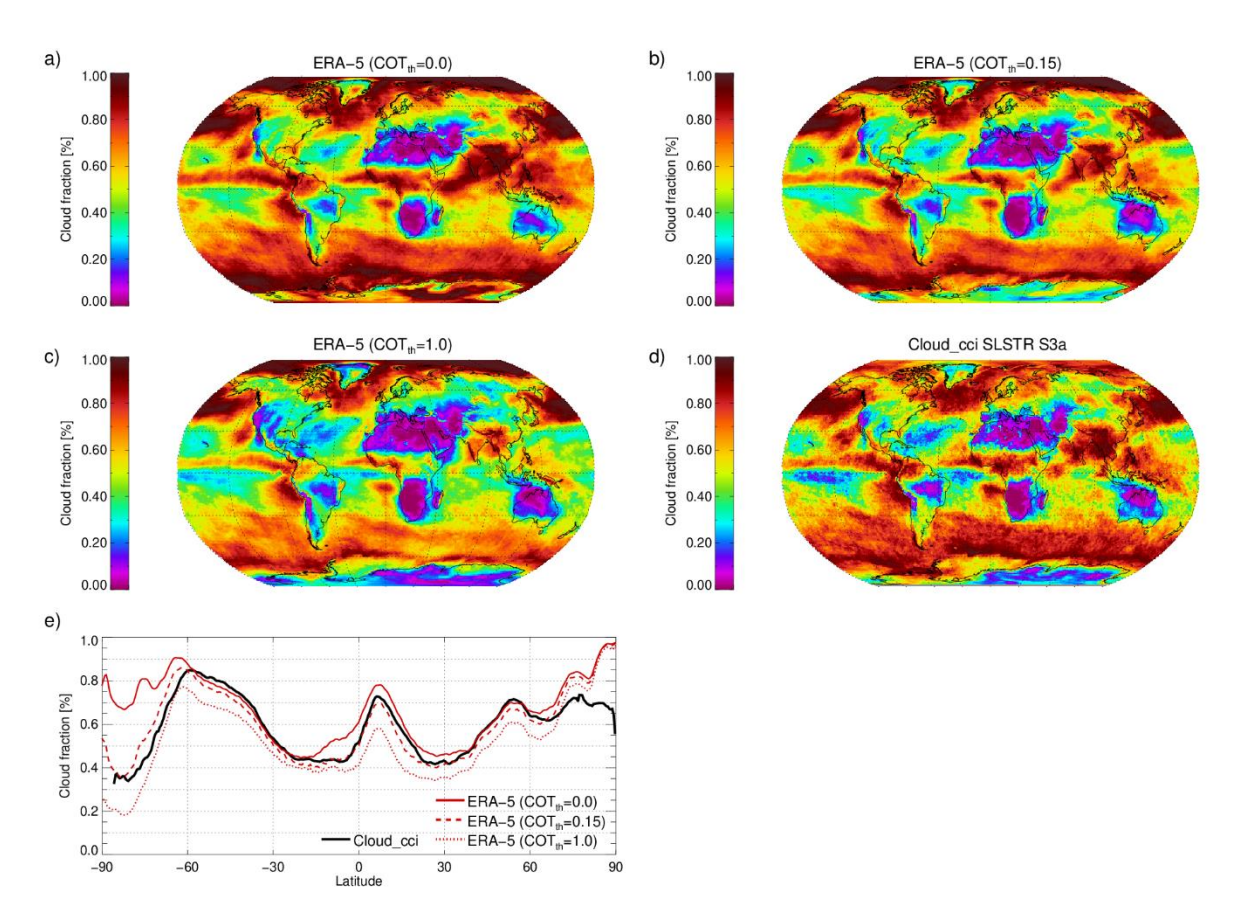
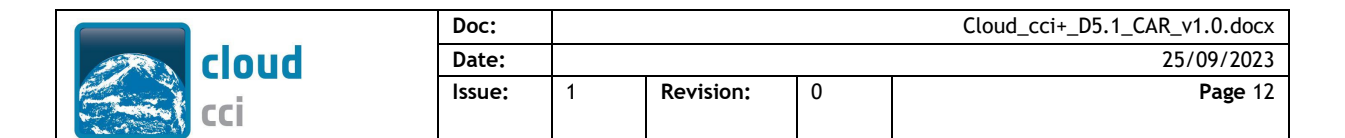


Figure 3-1 Monthly mean cloud fraction (CFC) from ERA-5 (a-c) and Cloud_cci+ v3 SLSTR S3a (d) for July 2019, where the ERA-5 cloud fraction was produced by SIMFERA for three optical thickness thresholds (COT_{th} = 0.0, 0.15, 1.0). Panel (e) is the zonal mean plot of CFC for all four sets. The uncertainty in Cloud_cci is mainly due to missing optically very thin clouds.

In Figure 3-2 the cloud fraction for low-, mid and high-level clouds are compared. The fraction of high-level clouds is much higher in ERA-5 than in SLSTR, which could point to a deficit in ERA-5 and/or to a lack of sensitivity to thin high-level clouds in SLSTR data. Removing cloud-top layers with an optical thickness below 1 brings the ERA-5 high-level cloud fraction down to SLSTR. For mid- and low-level clouds we generally see smaller values in ERA-5 compared to SLSTR, which is more pronounced for mid-level clouds.

Figure 3-3 depicts the relative frequency of cloud top pressure for SLSTR and ERA-5 stratified by cloud phase. While for liquid clouds the agreement between ERA-5 and SLSTR is reasonably (for all COT threshold), for ice clouds ERA-5 has clearly more high clouds (and less mid-level and low-level clouds) than SLSTR even when cloud top layers up to an optical thickness of 1 are removed from ERA-5. This confirms the findings for the cloud layer fractions above.

As last example, Figure 3-4 shows maps and zonal mean plots of monthly mean liquid cloud fraction. Between 50S and 50N the cloud phase agrees reasonably well, when no clouds layers are removed from ERA-5. Towards the higher latitudes, we find that ERA-5 has less liquid clouds than SLSTR, relatively speaking. Removing thin cloud top layers leads to generally increasing the liquid cloud fraction in ERA-5 by partly more than 20%.



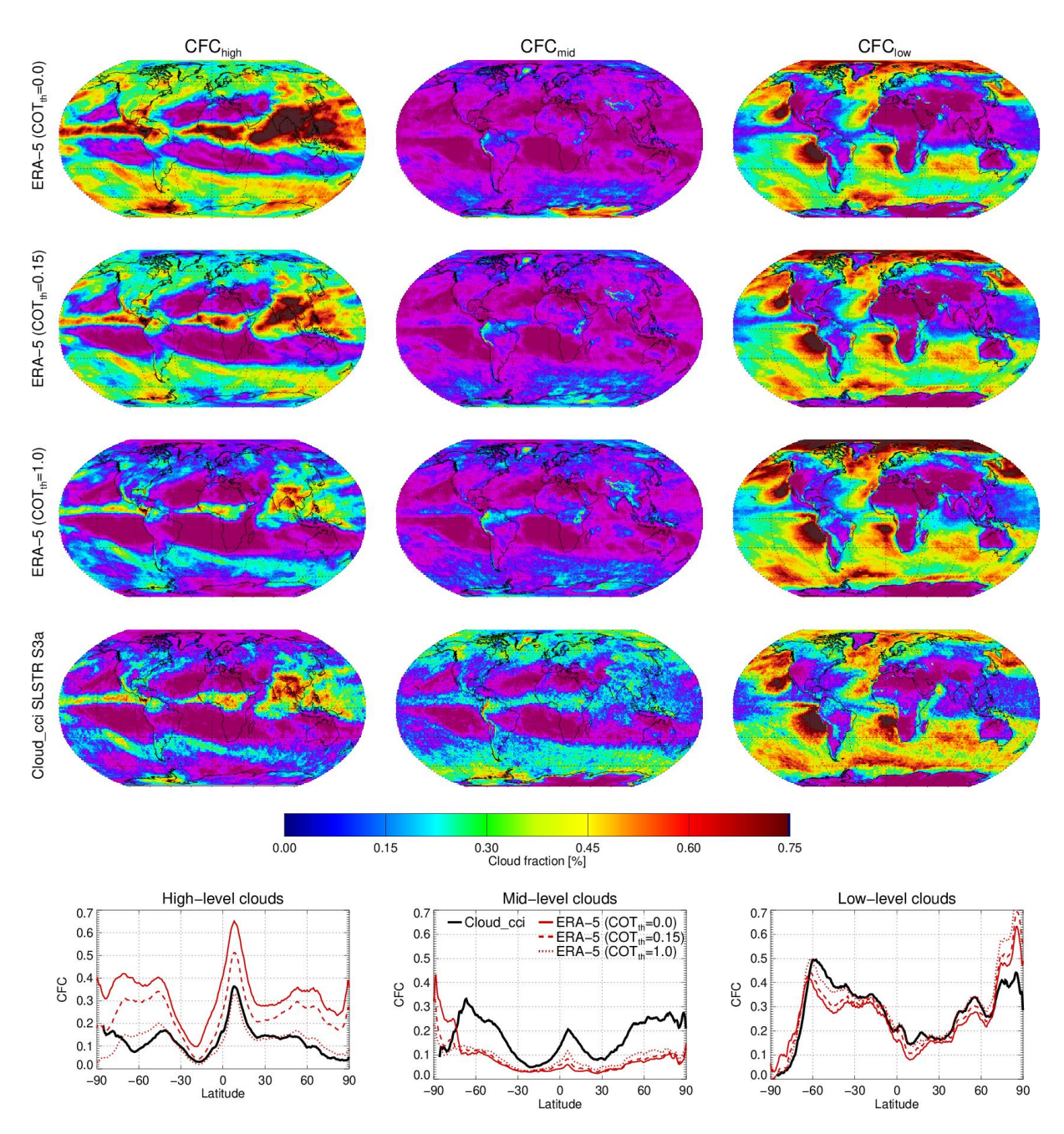
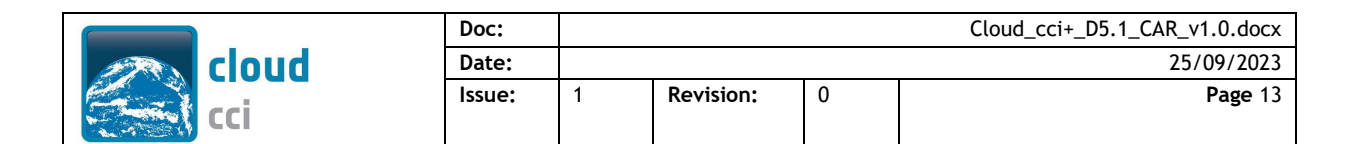


Figure 3-2 Monthly mean cloud fraction from ERA-5 (rows 1-3) and Cloud_cci+ v3 SLSTR S3a (row 4) for high-level (CFC_{high}, left column), mid-level (CFC_{mid}, middle column) and low-level clouds (CFC_{low}, right column) for July 2019. The ERA-5 cloud fraction was produced by SIMFERA for three optical thickness thresholds (COT_{th} = 0.0, 0.15, 1.0; rows 1 to 3, respectively). Bottom row: zonal mean plots for CFC_{high}, CFC_{mid} and CFC_{low}.



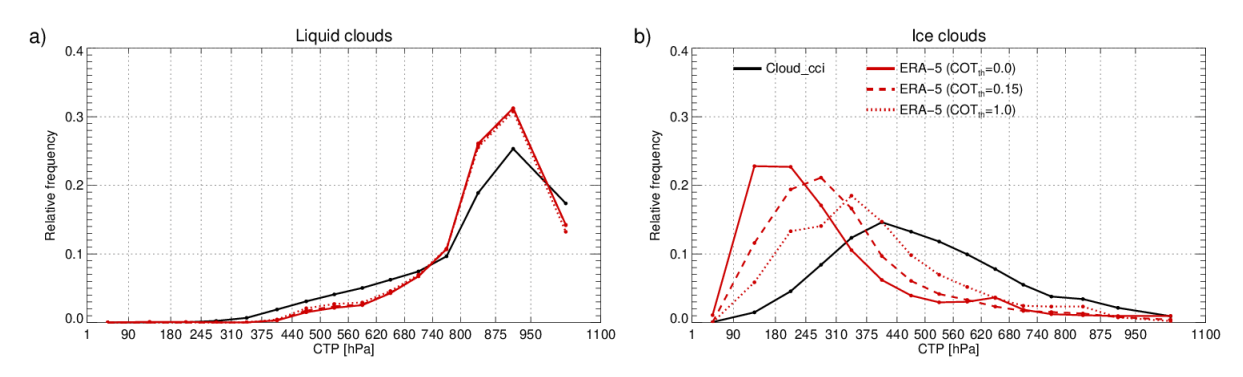


Figure 3-3 Global, relative frequency histograms of observed Cloud_cci cloud-top pressure (CTP) compared to ERA-5 CTP after applying SIMFERA with three COT thresholds COT_{th} (0.0, 0.15 and 1.00) - separated in liquid (a) and ice clouds (b) - for July 2019.

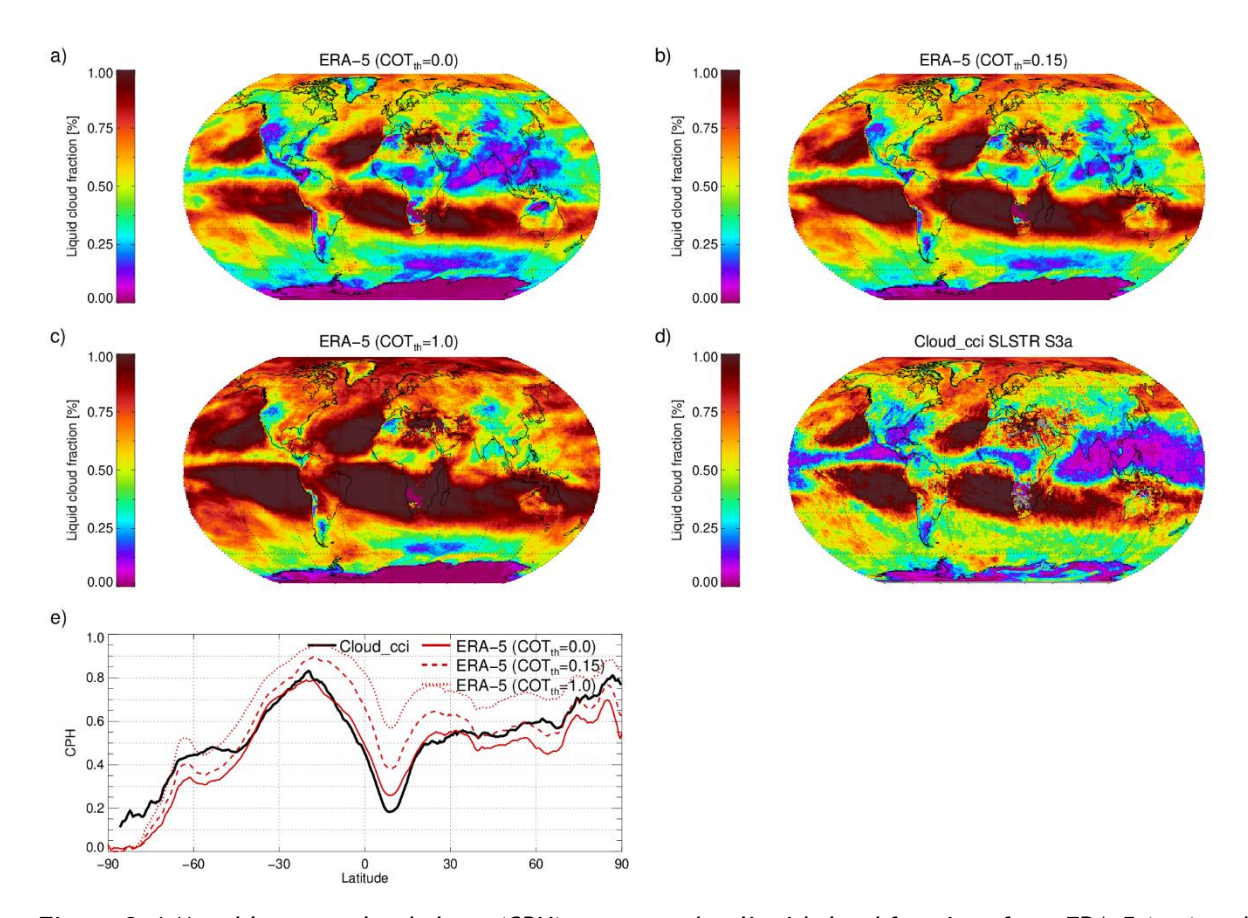


Figure 3-4 Monthly mean cloud phase (CPH), presented as liquid cloud fraction, from ERA-5 (a-c) and Cloud_cci+ v3 SLSTR S3a (d), where the ERA-5 liquid cloud fraction was produced by SIMFERA for three top-down optical thickness thresholds (COT_{th} = 0.0, 0.15, 1.0), at which the phase was collected from ERA-5 profiles. (e) Zonal mean plot of CPH for all four sets.



Doc:				Cloud_cci+_D5.1_CAR_v1.0.docx
Date:				25/09/2023
Issue:	1	Revision:	0	Page 14

4 Definitions, Acronyms, Abbreviations

AATSR	Advanced Along Track Scanning Radiometer			
ATBD	Algorithm Theoretical Basis Document			
ATSR	Along-Track Scanning Radiometer			
AVHRR	Advanced Very High Resolution Radiometer			
CEDA	British Atmospheric Data Centre			
BRDF	Bidirectional Reflectance Distribution Function			
CALIPSO	Cloud-Aerosol Lidar and Infrared Pathfinder Satellite Observations			
CFMIP	Cloud Feedback Model Intercomparison Project			
СМ	Configuration Management			
CMIP	Climate Model Intercomparison Project			
CM SAF	EUMETSAT Satellite Application Facility on Climate Monitoring			
COSP	CFMIP Observational Simulator Package			
DARDAR				
DISORT	Discrete Ordinates Radiative Transfer			
DWD	Deutscher Wetterdienst			
EC-EARTH	Earth system climate modelling version of the ECMWF model			
ECMWF	European Centre for Medium Range Weather Forecast			
ECSS	European Cooperation for Space Standardization			
ECV	Essential Climate Variable			
EO	Earth Observation			
EOS	Earth Observing System			
ESA	European Space Agency			
EUMETSAT	European Organization for the Exploitation of Meteorological Satellites			
FCDR	Fundamental Climate Data Record			
GCM	Global Circulation Model			
GCOS	Global Climate Observing System			
GERB	Geostationary Earth Observation Budget Instrument			
GEWEX	Global Energy and Water Cycle Experiment			
GRAPE	Global Retrieval of ATSR cloud Parameters and Evaluation			
GSICS	Global Space-based Inter-Calibration System			
GTS	Global Telecommunication System			
IPCC	International Panel on Climate Change			
IR	Infrared			
K	Kelvin			
MODIS	Moderate Resolution Imaging Spectroradiometer			
MSG	Meteosat Second Generation			
MTG	Meteosat Third Generation			
NASA	National Aeronautics and Space Administration			
NERC	Natural Environment Research Council			
CEDA	NERC Earth Observation Data Centre			
NetCDF	Network Common Data Form			



Doc:				Cloud_cci+_D5.1_CAR_v1.0.docx
Date:				25/09/2023
Issue:	1	Revision:	0	Page 15

NIR	Near Infrared			
NOAA	National Oceanic & Atmospheric Administration			
NWP	Numerical Weather Prediction			
OE	Optimal Estimation			
OLR	Outgoing Longwave Radiation			
ORAC	Oxford RAL Aerosol and Cloud			
UO	University of Oxford			
PUG	Product User Guide			
PVP	Product Validation Plan			
PVIR	Product Validation and Intercomparison Report			
RAL	Rutherford Appleton Laboratory			
RTM	Radiative Transfer Model			
RTTOV	Radiative Transfer for TOVS			
SAF	Satellite Application Facility			
SCOPE-CM	Sustained and Coordinated Processing of Environmental Satellite Data for Climate Monitoring			
SEVIRI	Spinning Enhanced Visible and Infrared Imager			
SLSTR	Sea and Land Surface Temperature Radiometer			
SOW	Statement Of Work			
SST	Sea Surface temperature			
SVR	System verification Report			
TCDR	Thematic Climate Data Record			
TIR	Thermal Infrared			
TR	Technical Requirement			
WCRP	World Climate Research Program			
WMO	World Meteorology Organisation			



Doc:				Cloud_cci+_D5.1_CAR_v1.0.docx
Date:				25/09/2023
Issue:	1	Revision:	0	Page 16

References

Jones W., Stengel M. Stier, P., A Lagrangian Perspective on the Lifecycle and Cloud Radiative Effect of Deep Convective Clouds Over Africa, 2023, in preparation

RUCS, 2020: ESA Cloud_cci+ Report on User Case Study 2: Designing a "Sunny Vacation Map" based on Satellite Observations on Clouds and Radiation, Issue: Issue 1 Revision 0, Released: 17.03.2021

Stengel, M., Schlundt, C., Stapelberg, S., Sus, O., Eliasson, S., Willén, U., and Meirink, J. F.: Comparing ERA-Interim clouds with satellite observations using a simplified satellite simulator, Atmos. Chem. Phys., 18, 17601-17614, https://doi.org/10.5194/acp-18-17601-2018, 2018.

Stengel, M., Stapelberg, S., Sus, O., Finkensieper, S., Würzler, B., Philipp, D., Hollmann, R., Poulsen, C., Christensen, M., and McGarragh, G.: Cloud_cci Advanced Very High Resolution Radiometer post meridiem (AVHRR-PM) dataset version 3: 35-year climatology of global cloud and radiation properties, Earth Syst. Sci. Data, 12, 41-60, https://doi.org/10.5194/essd-12-41-2020, 2020.

Stengel, M., Meirink, J. F., & Eliasson, S. (2023). On the temperature dependence of the cloud ice particle effective radius—A satellite perspective. Geophysical Research Letters, 50, e2022GL102521. https://doi.org/10.1029/2022GL102521